

## SYNTHESIS OF SOME NEW PYRAZOLE DERIVATIVES AS ANTIBACTERIAL AGENTS

Ahmed A. Nasser<sup>1,2</sup>, Sherif F. Hammad<sup>3</sup>, Abdelrahman S. Mayhoub<sup>1,2</sup>, Mohamed M. Elsebaei<sup>1\*</sup>.

<sup>1</sup>Department of Pharmaceutical Organic Chemistry, College of Pharmacy, Al-Azhar University, Cairo 11884, Egypt.

<sup>2</sup>University of Science and Technology, Nanoscience Program, Zewail City of Science and Technology, October Gardens, 6th of October, Giza 12578, Egypt.

<sup>3</sup>Basic and Applied Sciences Institute, Egypt-Japan University of Science and Technology (E-JUST), New Borg El-Arab City 21934, Alexandria, Egypt.

\*Corresponding author: [m.elsebaei@azhar.edu.eg](mailto:m.elsebaei@azhar.edu.eg)

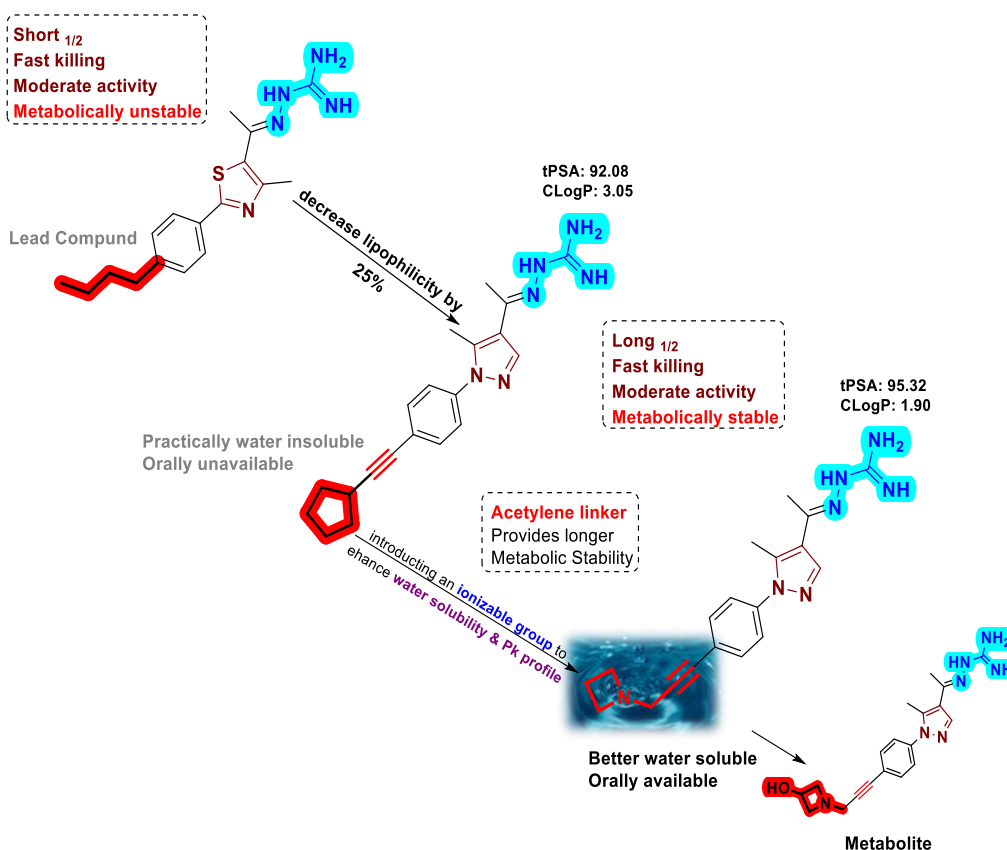
### ABSTRACT

Small organic phenylpyrazole scaffolds with high lipophilic properties are often associated with poor physicochemical properties, leading to more off-target actions and lower chances of full clinical trials. Therefore, we targeted the lipophilic tail of metabolically stable alkynylphenylpyrazole derivatives that exhibit remarkably high lipophilic properties and introduced a cyclic amine to improve their physicochemical characteristics. Alkynyl derivatives with 4-membered rings were the only ones that exhibited significant antibacterial activity. The azetidine moiety-containing compound 8 showed moderate antibacterial activity against MRSA. It significantly enhanced the water solubility and pharmacokinetic profile with an increase in the half-life and the time during which its plasma concentration was above its minimum inhibitory concentration against MRSA. The pharmacokinetic properties of the new series were successfully improved while the biological activity of the compounds against MRSA was maintained by the modifications of the alkynylphenylpyrazoles described here.

**Keywords:** *antibiotic resistance, MDR-bacteria, MRSA, cyclic amine, Sonogashira cross-coupling.*

## 1. Introduction

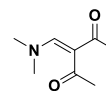
Antibiotic-resistant bacteria have been responsible for an increase in the prevalence of life-threatening infections globally.(Nathan 2020) The alarming rise in antibiotic resistance in global health requires extensive research to reduce this urgent problem. The most widespread cause of infections in hospitals and the community is methicillin-resistant *S. aureus* (MRSA).(Sugden, Kelly et al. 2016, Burnham, Leeds et al. 2017, Aljohani, El Zaloo et al. 2023) Egypt is among several Middle Eastern countries experiencing an increase in MRSA infections.(Eid, Elsebaei et al. 2017, Algammal, Hetta et al. 2020, Awaji, El Zaloo et al. 2024) The MRSA is the source of several hospital outbreaks due to resistance to  $\beta$ -lactam antibiotics, making the treatment of MRSA infections challenging. The emergence of drug-resistant *S. aureus* strains with intermediate susceptibility or resistance to vancomycin has significantly worsened the issue. The value of individual responsibility in combating antimicrobial resistance continues to rise as it approaches alarming levels.(Lee, De Lencastre et al. 2018, Turner, Sharma-Kuinkel et al. 2019) In 2014, (Mohammad, Mayhoub et al. 2014), our group discovered the promising phenylthiazole scaffold, which contains a thiazole core with an alkyl chain tail and a guanidine head. The two moieties are essential for their antibacterial activity and identified via the structure-activity relationship (SAR) studies.(El-Gamal, Sherbiny et al. 2015, Elsebaei, Mohammad et al. 2019, El-Din, Elsebaei et al. 2023, Elbakry, Harras et al. 2024) The research focus aims to enhance their activity, pharmacokinetics, and metabolic profile in addition to reducing the bacterial resistance. The narrow spectrum of the developed phenylthiazoles could be related to low permeability, which may limit access to intracellular target sites.(Elsebaei, Mohammad et al. 2018, Elsebaei, Abutaleb et al. 2019, Helal, Sayed et al. 2019, Mancy, Abutaleb et al. 2019, Hosny, Abutaleb et al. 2020, Elsebaei, Ezzat et al. 2024) However, we focused on the central thiazole ring and replaced it with the pyrazole ring, which represents a more polar azole moiety to reduce the lipophilicity and maintain the hydrogen bonding interactions with the bacterial membrane protein target. This minor modification suggests that reducing the lipophilicity by a factor of 25% can improve the bioavailability and pharmacokinetic profile.(Hammad, Abutaleb et al. 2019, Omara, Hagraas et al. 2023) In this study, we aimed to control the molecular obesity of alkynylphenylpyrazole derivatives by the insertion of a polar nitrogen atom into the lipophilic tail, which may balance the lipophilicity and hydrophilicity with optimizing the drug-like characteristics.

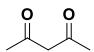


**Figure 1.** Summary of the objective phenylpyrazole scaffolds: Improvement of pharmacokinetic profile with promising antibacterial activity.

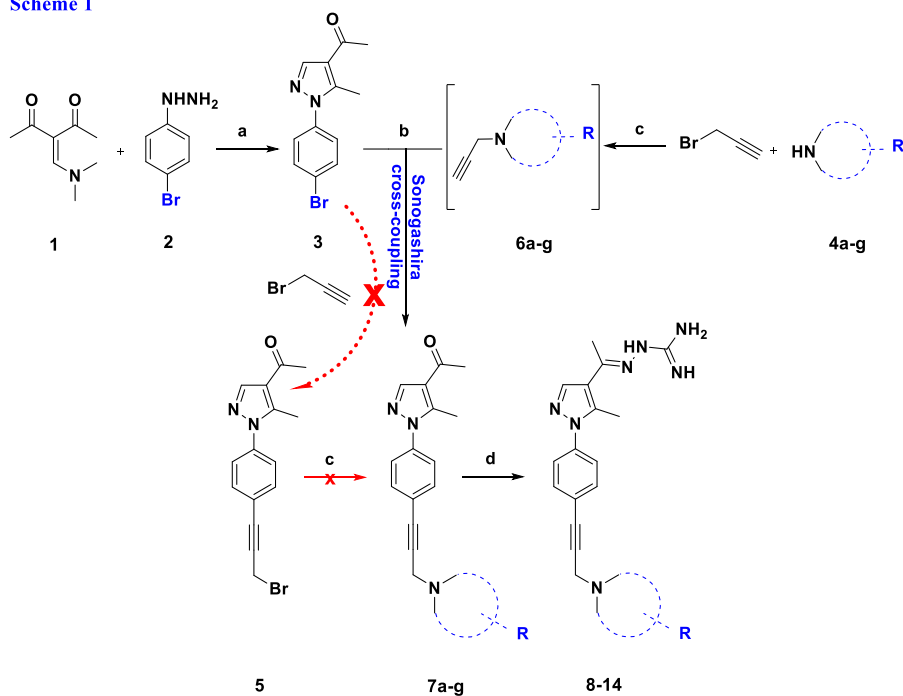
## 2. Result and Discussion




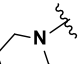
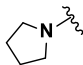
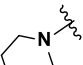
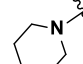
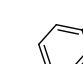
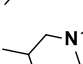
**2.1. Chemistry.** The reaction of 3-[(dimethylamino)methylene]pentane-2,4-dione



(1), synthesized *in situ* from  acetylacetone and dimethylformamide dimethylacetal, with p-bromophenylhydrazine (2) yielded the starting building block *N*-phenylpyrazole (3) (Scheme 1). In addition, the cyclic *N*-propargyl amines **6a-g** were first prepared and then allowed to react with the bromo phenylpyrazole intermediate **3** under the same standard Sonogashira cross-coupling conditions to give the intermediate acetyl compounds **7a-g**. The subsequent reaction with aminoguanidine in the presence of a catalytic amount of hydrochloric acid provided the final products **8-14** (Scheme 1).

Scheme 1



Comp	HN  -R	Comp	HN  -R
4a, 6a, 7a, 8		4e, 6e, 7e, 12	
4b, 6b, 7b, 9		4f, 6f, 7f, 13	
4c, 6c, 7c, 10		4g, 6g, 7g, 14	
4d, 6d, 7d, 11			

**Reagents and conditions:** (a) Absolute EtOH, heat to reflux, 12 h; (b) comp (6a-g), PdCl<sub>2</sub>(PPh<sub>3</sub>)<sub>2</sub> (5% mol), CuI (7.5% mol), Et<sub>3</sub>N, DME, heat at 50 °C for 24 h; in a sealed flask; (c) anhydrous K<sub>2</sub>CO<sub>3</sub>, DME, heat at 110 °C for 4 h; (d) aminoguanidine HCl, EtOH, conc. HCl, heat to reflux, 3 h.

## 2.2. Biological Results and Discussion.

**2.2.1. Antibacterial activity.** The initial screening of the new compounds against MRSA USA300, *Clostridium difficile* (*C. difficile*), *Escherichia coli* (*E. coli*), and *Neisseria gonorrhoeae* (*N. gonorrhoeae*) are the clinically most important MDR pathogens that showed a broad spectrum of antibacterial activity, with MIC values ranging from 4 to over 32 µg/mL (Table 1-2).

Generally, the new derivatives belong to the alkynylphenylpyrazole scaffolds in the series. The results showed the importance of side chain size in optimizing antibacterial activity for alkynylphenylpyrazole derivatives. None of derivatives showed promising activity except the one with small cyclic amines consisting of a 4-membered ring, which showed moderate antibacterial activity against MRSA USA300. The azetidine moiety-containing compound **8** was the most potent side chain with an MIC value of 4  $\mu\text{g/mL}$ . The inactive derivatives indicate that the active site of the target is unable to accommodate the bulky side chains, especially those with greater than 4 carbon atoms. The SAR appears clear that the activity correlates strongly with the ring size on the nitrogen atom of the side chain. Briefly, the elongation of the nitrogen-containing side chain lacks antibacterial activity. Linezolid was used as a positive control in the antibacterial evaluation against MRSA USA300 with an MIC of 1  $\mu\text{g/mL}$ .

**Table 1.** Antibacterial activity (MICs and MBCs in  $\mu\text{g/mL}$ ) of alkynylphenylpyrazole derivatives against a panel of clinically important Gram-positive bacterial strains.

Compounds/ control antibiotics	Bacterial Strains (Gram-positive)			
	<i>S. aureus</i> NRS384 (MRSA USA300)		<i>C. difficile</i> ATCC-BAA 1870	
	MIC	MBC	MIC	MBC
<b>8</b>	4	4	32	32
<b>9</b>	> 64	> 64	> 64	> 64
<b>10</b>	64	64	64	64
<b>11</b>	32	> 64	64	> 64
<b>12</b>	64	> 64	> 64	> 64
<b>13</b>	> 64	> 64	> 64	> 64
<b>14</b>	64	> 64	64	> 64
Linezolid	1	16	NT	NT
Vancomycin	1	1	1	1

**Table 2.** Antibacterial activity (MICs and MBCs in  $\mu\text{g/mL}$ ) of alkynylphenylpyrazole derivatives against a panel of clinically important Gram-negative bacterial strains.

Compounds/ control antibiotics	Bacterial Strains (Gram-negative)		
	<i>E. coli</i> BW 25113		<i>N. gonorrhoeae</i> FA1090
	MIC	MBC	MBC
<b>8</b>	> 64	> 64	64
<b>9</b>	> 64	> 64	> 64
<b>10</b>	> 64	> 64	> 64
<b>11</b>	64	> 64	> 64
<b>12</b>	> 64	> 64	> 64
<b>13</b>	> 64	> 64	> 64
<b>14</b>	> 64	> 64	> 64
Gentamicin	0.25	0.25	NT
Ceftriaxone	NT	NT	0.008

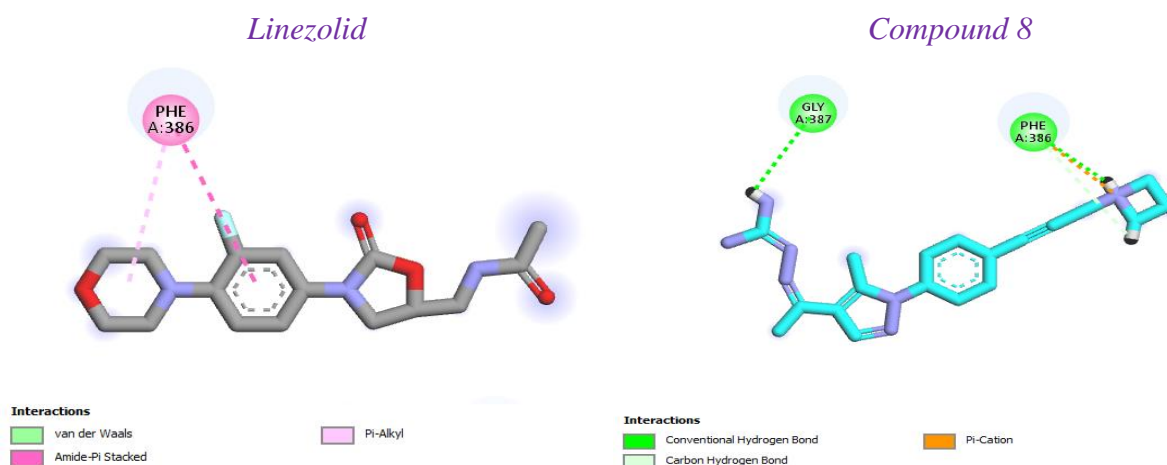
### 2.3. Docking Study.

A docking study was performed on the synthesized compound at the binding sites of the crystal structure of the AcrB complexed with linezolid at 3.5 resolution (PDB: 4K7Q) to investigate the mode of interaction with the desired target. Docking simulation showed that the compound has high binding affinity toward this target. The molecular docking protocol was implemented using MOE 14.0 software. The target membrane protein was prepared, and the active binding site was identified *via* the position coordinates of the cocrystallized ligand. The results of the docking protocol were verified by redocking the cocrystallized linezolid into the active site of the target. The docking approach was validated as the root mean square deviation (RMSD) between cocrystallized conformers of linezolid and redocked conformers was 0.90.

In order to initially understand the mechanism of action of this scaffold, we performed a quick docking study using ArcB. The ArcB is a principal multidrug efflux transporter widely distributed in *E. coli* and other gram-negative bacteria. (Hung, Kim et al. 2013, Ornik-Cha, Wilhelm et al. 2021) The reason we selected this target is the availability of structurally similar molecules (linezolid, for instance) that bind to this target. We understand that this may not be the ideal target to hit in our case, but the activity of our molecule **1y** against *E. coli* encouraged us to pursue this target.

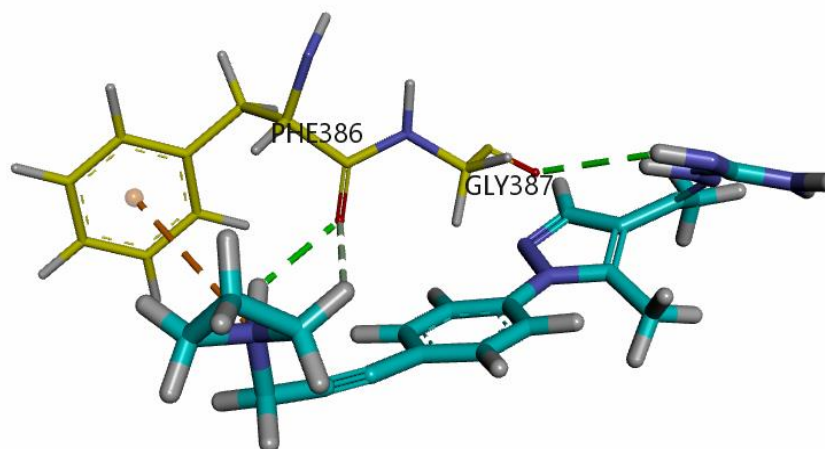
The docking analysis revealed that our compound **8** kept the same binding pattern as linezolid (**Figure 2**), which includes hydrogen bonding between the nitrogen atom of the azetidine moiety and PHE 386. Interestingly, our molecule was able to engage another binding represented by the hydrogen bonding between the aminoguanidine nitrogen and GLY 387. Thus, data revealed that ArcB may be the target of these molecules. However, due to the controversial activity against *E. coli* between the lead and our molecules, further studies to confirm the mechanism of action are warranted.

Linezolid was the first oxazolidinone antibiotic approved by the FDA. (Elsebaie, El-Din et al. 2022, Sayed, Abutaleb et al. 2023, Shahin, Mohamed et al. 2023) The mechanisms associated with bacterial resistance to naturally occurring antibiotics are not related to linezolid, as it is a synthetic compound. The binding mode of the cocrystallized ligand exhibited a binding energy of  $-4.34 \text{ kcal mol}^{-1}$ . In detail, the crystal structure of an AcrB-linezolid complex was determined at a resolution of 3.5 Å. The linezolid binds to the A385/F386 loop of each protomer in the symmetric trimer, as the structure shows. Ampicillin and nafcillin have previously been shown to interact with this loop. A loop at the deepest point of the periplasmic cleft exhibits a conformational shift that is thought to be important for AcrA binding and drug transport.

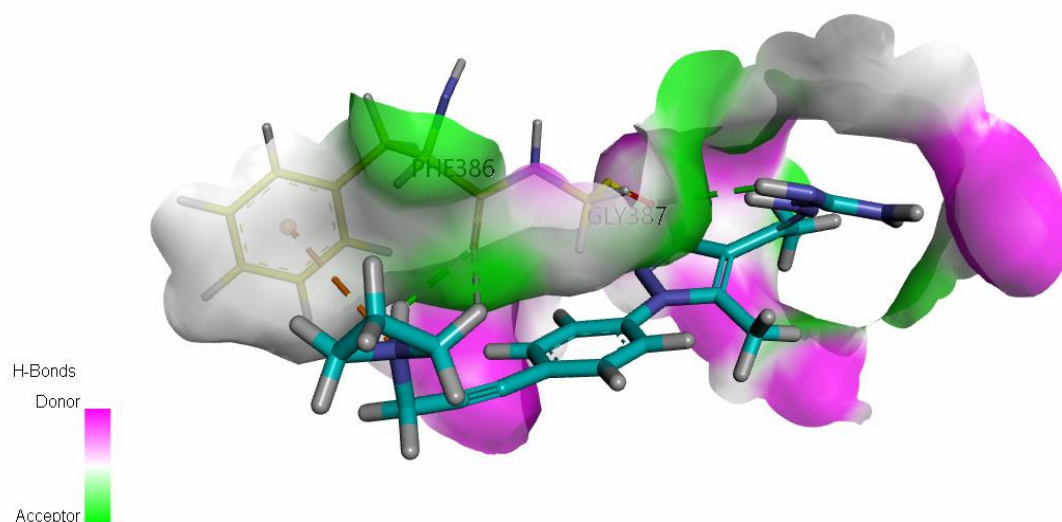


**Figure 2.** 2D superimposition images of the redocked conformers of linezolid and compound **8** with RMSD scores of 1.91 and 2.08.

The *N*-3-fluoro-4-(morpholin-4-yl)phenyl group of the linezolid drug formed an interaction with this membrane protein AcrB, with the morpholine moiety forming a pi-alkyl interaction with PHE386. The phenyl ring moiety binds to the same amino acid, PHE386, via one amide pi-stacked interaction. Compound **8** exhibited a binding mode similar to that of the reference linezolid. It showed an affinity value of  $-5.15 \text{ kcal mol}^{-1}$ .



**Figure 3.** Binding analysis of compound **8** within AcrB active site: Visualization of hydrogen bonds (green lines) and pi interactions (orange lines).



**Figure 4.** Mapping surface showing compound **8** occupying the AcrB active pocket.

The azetidine moiety enhances the water solubility and pharmacokinetic profile as a morpholine moiety in the structure of linezolid and forms two hydrogen bonds: one conventional hydrogen bond with a distance of 2.29 Å and one carbon-hydrogen bond with a distance of 2.93 Å, and some pi-cation interactions with the same amino acid as the reference ligand PHE386. Furthermore, the aminoguanidine moiety forms a hydrogen bond with GLY387 with a distance of 2.74 Å. Such extra hydrogen bonding interactions may explain the higher activity of this compound compared to the standard compound.

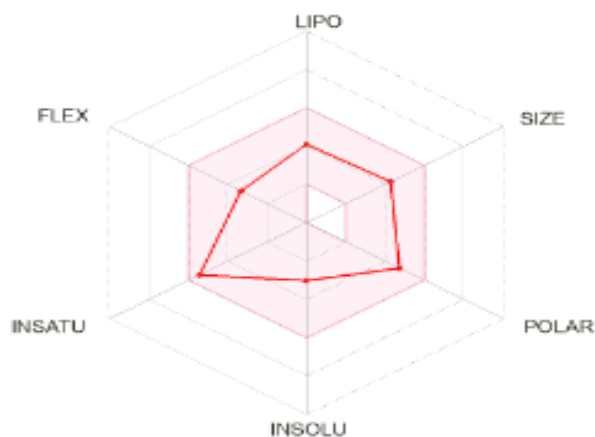
#### 2.4. Pharmacokinetics Study.

The development of drug discovery requires the ability to predict pharmacokinetics, pharmacodynamics, and drug-likeness profiles. It gives pharmaceutical companies the best advantage achievable or perhaps inspires others to continue the struggle. Over the last two decades, online tools and software have become available to predict absorption, distribution, metabolism, and excretion (ADME). After collecting the antibacterial data, compound **8** was selected to test the hypothesis before conducting more detailed in silico studies to see whether the new chemical modification proposed in this work would improve the overall PK profile of the phenylpyrazole compounds. It is worth noting that the alkynyl derivative of compound **1y** was not orally available and had water solubility problems. In this study, the properties of the best candidate were calculated, and the results were summarized in (Tables 3-4).

SwissADME was the software of choice for PK profile prediction. The most suitable parameter to assess the impact of molecular rigidity on oral bioavailability was the number of rotatable bonds. Generally, the number of rotatable bonds corresponds to the molecular weight. Our candidates have a molecular weight of less than 500 and a cLogP of less than 5, indicating that they initially have good oral bioavailability. Further division was

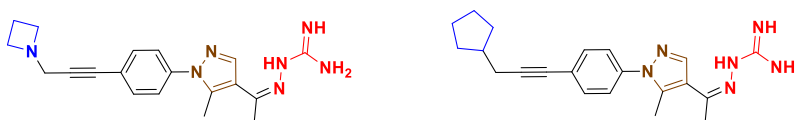


made by dividing the number of rotatable bonds. This number illustrates the oral bioavailability and determines the flexibility of the molecule. It can be calculated by counting the number of non-ring bonds that are not attached to the terminal or a hydrogen atom. According to our analysis, compound **8** has less than 7 rotatable bonds, indicating good bioavailability. The number of H-bond acceptors and donors is less than 5. As a result, it is conceivable that this compound has good absorption.



**Figure 5.** Egg radar of the most active compound **8**

**Table 3.** Key physicochemical properties of compound **8** and **1y** prediction via SwissADME.



Compound	Compound <b>8</b>		Previously Prepared Compound <b>1y</b>			
	tPSA	HBD	HBA	NORTB	M.W	LogP
<b>8</b>	95.32	3	4	5	349.43	1.90
<b>1y</b>	92.08	3	3	4	348.44	3.05

The physicochemical property measurements indicate that compound **8** has optimal properties for oral therapeutic administration. To estimate the permeability of polar atoms *via* membranes, we determined the tPSA; its value is 95.32 Å<sup>2</sup>, and its cLogP is 1.90. Notably, the tPSA value of compound **8** is extremely close to that of lead compound **1y**,

which has almost the same number of carbon atoms. Just inserting a nitrogen atom into the lipophilic side chain of compound **1y** significantly reduces its cLogP value by about half. So, this led to an improvement in the water solubility of compound **8**.

**Table 4.** Predicting the drug-likeness of compound **8** via Molsoft.

Solubility (mg/L)	Drug Likeness model score	Lipinski's rule violation	Bioavailability score
0.19	0.87	0	0.55

The probability that drug candidates will have the chemical and physical properties required for their oral bioavailability can be predicted via Lipinski's rule. This rule is used in drug discovery through the physicochemical properties to predict pharmacokinetic drug features. According to Lipinski's rule of five, oral bioavailability of a biologically active molecule must not have more than one violation of these criteria. The azetidine-containing compound **8** satisfied Lipinski's rule for drug likeness. For this reason, we believe it has good oral bioavailability and can enhance aqueous solubility.

### 3. Conclusion

There is a statistically significant relationship between the physicochemical properties of drug candidates and attrition from clinical trials. Therefore, physicochemical properties influence the pharmacokinetic profile of the drug. Poor physicochemical properties lead to suboptimal bioavailability, which increases the chance that a drug candidate will fail to advance via later stages of clinical trials. To develop the phenylpyrazole scaffolds, the insertion of a nitrogen-containing ring in the lipophilic moiety of phenylpyrazole molecules regulates their lipophilic-hydrophilic balance due to nitrogen atoms increasing polarity and enhancing hydrogen-bonding interactions with bacterial targets, which may improve aqueous solubility. Additionally, the alkynyl-containing phenylpyrazole derivatives enhance the metabolic stability.

Briefly, the cLogP value of the azetidine-containing derivative was reduced to half the value of the corresponding derivative **1y** with ~ the same number of carbons, which significantly improved its aqueous solubility and oral bioavailability. Another advantage of the PK profile is that the hydroxy azetidine derivative as the main primary metabolite plays a vital role in the drug's potency, which can contribute to prolonged antibacterial activity. Consequently, this work shows that the azetidine-containing compound is a promising therapeutic candidate for *S. aureus* infections, notably those associated with biofilms.

## Experimental

### 4.1. Chemistry

General. All biologically tested compounds have a purity of 98% or more.  $^1\text{H}$  NMR spectra were run at 400 MHz, and  $^{13}\text{C}$  NMR spectra were determined at 100 MHz in deuterated dimethyl sulfoxide (DMSO-*d*6) on a Varian Mercury VX-400 NMR spectrometer. Chemical shifts are given in parts per million (ppm) on the delta ( $\delta$ ) scale. Chemical shifts were calibrated relative to those of the solvents. Column chromatography was performed on 230-400 mesh silica. The progress of reactions was monitored with Merck silica gel IB2-F plates (0.25 mm thickness). Melting points were determined using capillary tubes with a Stuart SMP30 apparatus and are uncorrected. All yields reported refer to isolated yields. Compound (3) was prepared as reported (Mohammad, Mayhoub et al. 2014).

#### 1-(5-Methyl-1-(4-(substituted alkynyl)phenyl)-1H-pyrazol-4-yl)ethenone (7a-g).

*General procedure:* To dry DMF (5 mL) in a round flask were added appropriate sec. amines **4a–g** (200 mg, 1.5–2 mmol), propargyl bromide (476 mg, 300  $\mu\text{L}$ , 3–4 mmol, 2 equiv.), and anhydrous potassium carbonate (830 mg, 4.5–6 mmol, 3 equiv.); the mixture was then heated at 110  $^\circ\text{C}$  and stirred for 4 h to afford compounds **6a–g**. Next, the reaction mixture was taken without purification and added to a 75-mL sealed tube charged with compound **3** (300 mg, 0.87 mmol) in dry DME (10 mL) and triethylamine (2 mL). After the reaction mixture was purged with dry nitrogen gas for 15 min, dichlorobis-(triphenylphosphine)palladium(II) (46 mg, 0.065 mmol) and copper(I) iodide (33 mg, 0.17 mmol) were added. The sealed tube was then maintained at 50  $^\circ\text{C}$  for 24 h, and the reaction progress was monitored by TLC. After completion of the reaction, the reaction mixture was passed through a pad of silica gel with DCM (50 mL). Organic materials were then collected, concentrated under vacuum, and purified using silica gel chromatography (DCM/methanol 98:2). Physical properties, yields, and characterization data of isolated products are listed below.

#### 1-(1-(4-(3-(Azetidin-1-yl)prop-1-yn-1-yl)phenyl)-5-methyl-1H-pyrazol-4-yl)ethan-1-one (7a).

Brown oil (121 mg, 74.2%);  $^1\text{H}$  NMR (DMSO-*d*6)  $\delta$ : 8.05 (s, 1H), 7.71 (d,  $J = 8.2$  Hz, 2H), 7.15 (d,  $J = 8.2$  Hz, 2H), 3.45 (s, 2H), 3.08 (t,  $J = 8.0$  Hz, 4H), 2.45 (s, 3H), 2.38 (s, 3H), 1.65–1.58 (m, 2H);  $^{13}\text{C}$  NMR (DMSO-*d*6)  $\delta$ : 195.8, 147.7, 145.8, 142.5, 138.3, 132.5, 127.5, 123.6, 122.7, 89.4, 81.6, 55.1, 42.1, 30.7, 18.6, 14.26; MS ( $m/z$ ); 293 ( $M^+$ , 100.00%).

**1-(5-Methyl-1-(4-(3-(pyrrolidin-1-yl)prop-1-yn-1-yl)phenyl)-1H-pyrazol-4-yl)ethan-1-one (7b).**

Brown oil (105 mg, 68.2%);  $^1\text{H}$  NMR (DMSO-*d*6)  $\delta$ : 8.03 (s, 1H), 7.68 (d,  $J$  = 8.2 Hz, 2H), 7.12 (d,  $J$  = 8.2 Hz, 2H), 3.42 (s, 2H), 3.12-3.01 (m, 4H), 2.41 (s, 3H), 2.37 (s, 3H), 1.85-1.78 (m, 4H);  $^{13}\text{C}$  NMR (DMSO-*d*6)  $\delta$ : 196.8, 147.3, 144.8, 141.5, 138.2, 132.1, 127.3, 122.6, 120.7, 87.4, 82.6, 54.1, 41.1, 29.7, 18.2, 13.26; MS ( $m/z$ ); 307 ( $M^+$ , 100.00%).

**1-(5-methyl-1-(4-(3-(4-methylpiperidin-1-yl)prop-1-yn-1-yl)phenyl)-1H-pyrazol-4-yl)ethan-1-one (7c).** Yellow oil (115 mg, 72%);  $^1\text{H}$  NMR (DMSO-*d*6)  $\delta$ : 8.08 (s, 1H), 7.73 (d,  $J$  = 8.2 Hz, 2H), 7.12 (d,  $J$  = 8.2 Hz, 2H), 3.62 (s, 2H), 2.68-2.57 (m, 4H), 2.39 (s, 3H), 2.32 (s, 3H), 1.65-1.57 (m, 5H), 0.92 (d,  $J$  = 6.2 Hz, 3H);  $^{13}\text{C}$  NMR (DMSO-*d*6)  $\delta$ : 196.4, 146.3, 144.5, 141.5, 138.2, 132.6, 127.3, 123.2, 122.7, 86.4, 81.4, 52.1, 42.1, 33.8, 30.7, 19.2, 12.26; MS ( $m/z$ ); 335 ( $M^+$ , 100.00%).

**1-(5-Methyl-1-(4-(3-(3-methylpiperidin-1-yl)prop-1-yn-1-yl)phenyl)-1H-pyrazol-4-yl)ethan-1-one (7d).** Yellow oil (109 mg, 71%);  $^1\text{H}$  NMR (DMSO-*d*6)  $\delta$ : 8.08 (s, 1H), 7.73 (d,  $J$  = 8.2 Hz, 2H), 7.12 (d,  $J$  = 8.2 Hz, 2H), 3.62 (s, 2H), 2.68-2.57 (m, 4H), 2.39 (s, 3H), 2.32 (s, 3H), 1.65-1.57 (m, 5H), 0.94 (d,  $J$  = 6.2 Hz, 3H);  $^{13}\text{C}$  NMR (DMSO-*d*6)  $\delta$ : 196.4, 146.3, 144.5, 141.5, 138.2, 132.6, 127.3, 123.2, 122.7, 86.4, 81.4, 52.1, 42.1, 33.8, 30.7, 19.2, 12.26; MS ( $m/z$ ); 335 ( $M^+$ , 100.00%).

**1-(5-Methyl-1-(4-(3-(2-methylpiperidin-1-yl)prop-1-yn-1-yl)phenyl)-1H-pyrazol-4-yl)ethan-1-one (7e).** Yellow oil (100 mg, 69%);  $^1\text{H}$  NMR (DMSO-*d*6)  $\delta$ : 8.08 (s, 1H), 7.73 (d,  $J$  = 8.2 Hz, 2H), 7.12 (d,  $J$  = 8.2 Hz, 2H), 3.62 (s, 2H), 2.68-2.57 (m, 4H), 2.39 (s, 3H), 2.32 (s, 3H), 1.65-1.57 (m, 5H), 0.94 (d,  $J$  = 6.2 Hz, 3H);  $^{13}\text{C}$  NMR (DMSO-*d*6)  $\delta$ : 196.4, 146.3, 144.5, 141.5, 138.2, 132.6, 127.3, 123.2, 122.7, 86.4, 81.4, 52.1, 42.1, 33.8, 30.7, 19.2, 12.26; MS ( $m/z$ ); 335 ( $M^+$ , 100.00%).

**1-(5-Methyl-1-(4-(3-(piperidin-1-yl)prop-1-yn-1-yl)phenyl)-1H-pyrazol-4-yl)ethan-1-one (7f).** Yellow oil (120 mg, 74%);  $^1\text{H}$  NMR (DMSO-*d*6)  $\delta$ : 8.08 (s, 1H), 7.73 (d,  $J$  = 8.2 Hz, 2H), 7.12 (d,  $J$  = 8.2 Hz, 2H), 3.62 (s, 2H), 2.68-2.57 (m, 4H), 2.39 (s, 3H), 2.32 (s, 3H), 1.65-1.57 (m, 6H);  $^{13}\text{C}$  NMR (DMSO-*d*6)  $\delta$ : 196.4, 146.3, 144.5, 141.5, 138.2, 132.6, 127.3, 123.2, 122.7, 86.4, 81.4, 52.1, 42.1, 33.8, 30.7, 19.2, 12.26; MS ( $m/z$ ); 321 ( $M^+$ , 100.00%).

**1-(1-(4-(3-((4-hydroxyphenyl)amino)prop-1-yn-1-yl)phenyl)-5-methyl-1H-pyrazol-4-yl)ethan-1-one (7g).** Yellow oil (130 mg, 79%);  $^1\text{H}$  NMR (DMSO-*d*6)  $\delta$ : 9.14 (brs, 1H), 8.08 (s, 1H), 7.74 (d,  $J$  = 8.2 Hz, 2H), 7.24 (d,  $J$  = 8.2 Hz, 2H), 7.17 (d,  $J$  = 8.2 Hz, 2H), 6.94 (d,  $J$  = 8.2 Hz, 2H), 4.65 (brs, 1H), 3.62 (s, 2H), 2.39 (s, 3H), 2.32 (s, 3H);  $^{13}\text{C}$  NMR (DMSO-*d*6)  $\delta$ : 197.4, 157.3, 146.3, 148.3, 144.5, 141.3, 138.5, 132.6, 127.3, 123.3, 122.2, 120.2, 115.2, 86.4, 81.4, 32.8, 30.1, 12.26; MS ( $m/z$ ); 345 ( $M^+$ , 100.00%).

**2-(1-(5-Methyl-1-(4-(substituted)phenyl)-1H-pyrazol-4-yl)-ethylidene)hydrazine**

**Carboximidamide (8-14).** *General procedure:* Pyrazole derivatives (**7a–g**, 0.63 mmol) were dissolved in absolute ethanol (10 mL), aminoguanidine hydrochloride (70 mg, 0.63 mmol), and hydrochloric acid (0.1 mL). The reaction mixture was refluxed for 12 hours. The solvent was concentrated under reduced pressure, poured onto crushed ice, and neutralized with sodium carbonate (to pH 7-8). The solid precipitate was collected by filtration and washed with plenty of water. Crystallization from diethyl ether afforded the desired products as solids. Yields, physical properties, and spectral data of the isolated purified products are listed below.

**2-(1-(1-(4-(3-(Azetidin-1-yl)prop-1-yn-1-yl)phenyl)-5-methyl-1H-pyrazol-4-yl)ethylidene) hydrazine-1-carboximidamide (8).**

White solid (93 mg, 85.6%); mp = 175-177 °C. <sup>1</sup>H NMR (DMSO-*d*<sub>6</sub>) δ: 8.05 (s, 1H), 7.71 (d, *J* = 8.2 Hz, 2H), 7.15 (d, *J* = 8.2 Hz, 2H), 5.64 (brs, 4H), 3.45 (s, 2H), 3.08 (t, *J* = 8.0 Hz, 4H), 2.45 (s, 3H), 2.38 (s, 3H), 1.65-1.58 (m, 2H); <sup>13</sup>C NMR (DMSO-*d*<sub>6</sub>) δ: 153.8, 149.7, 141.8, 140.5, 138.2, 132.6, 127.5, 123.6, 122.7, 89.4, 81.6, 55.1, 42.1, 26.3, 18.6, 14.26; MS (*m/z*); 349 (M<sup>+</sup>, 100.00%). Anal. Calc. for: C<sub>19</sub>H<sub>23</sub>N<sub>7</sub> (349): C, 65.31; H, 6.63; N, 28.06; found; C, 65.37; H, 6.68; N, 28.01%. HPLC RT: 23.133; Area 98.33%.

**2-(1-(5-methyl-1-(4-(3-(pyrrolidin-1-yl)prop-1-yn-1-yl)phenyl)-1H-pyrazol-4-yl)ethylidene) hydrazine-1-carboximidamide (9).**

Yellow solid (98 mg, 87.6%); mp = 185-186 °C. <sup>1</sup>H NMR (DMSO-*d*<sub>6</sub>) δ: 8.03 (s, 1H), 7.68 (d, *J* = 8.2 Hz, 2H), 7.12 (d, *J* = 8.2 Hz, 2H), 5.74 (brs, 4H), 3.42 (s, 2H), 3.12-3.01 (m, 4H), 2.41 (s, 3H), 2.37 (s, 3H), 1.85-1.78 (m, 4H); <sup>13</sup>C NMR (DMSO-*d*<sub>6</sub>) δ: 153.7, 146.7, 141.8, 139.5, 138.2, 132.6, 127.5, 123.6, 122.7, 89.4, 81.6, 53.1, 41.1, 27.3, 19.6, 15.26; MS (*m/z*); 363 (M<sup>+</sup>, 100.00%). Anal. Calc. for: C<sub>20</sub>H<sub>25</sub>N<sub>7</sub> (363): C, 66.07; H, 6.93; N, 26.98; found; C, 66.11; H, 6.99; N, 26.91%. HPLC RT: 24.153; Area 97.43%.

**2-(1-(5-Methyl-1-(4-(3-(4-methylpiperidin-1-yl)prop-1-yn-1-yl)phenyl)-1H-pyrazol-4-yl) ethylidene)hydrazine-1-carboximidamide (10).**

Yellowish-white solid (105 mg, 89.6%); mp = 189-201 °C. <sup>1</sup>H NMR (DMSO-*d*<sub>6</sub>) δ: 8.08 (s, 1H), 7.73 (d, *J* = 8.2 Hz, 2H), 7.12 (d, *J* = 8.2 Hz, 2H), 6.44 (brs, 4H), 3.62 (s, 2H), 2.68-2.57 (m, 4H), 2.39 (s, 3H), 2.32 (s, 3H), 1.65-1.57 (m, 5H), 0.92 (d, *J* = 6.2 Hz, 3H); <sup>13</sup>C NMR (DMSO-*d*<sub>6</sub>) δ: 154.3, 147.7, 142.8, 140.5, 138.2, 132.6, 127.5, 123.6, 122.7, 89.4, 81.6, 52.1, 41.1, 32.5, 29.3, 25.9, 19.6, 15.26; MS (*m/z*); 391 (M<sup>+</sup>, 100.00%). Anal. Calc. for: C<sub>22</sub>H<sub>29</sub>N<sub>7</sub> (391): C, 67.49; H, 7.47; N, 25.04; found; C, 68.06; H, 7.58; N, 24.97%. HPLC RT: 25.296; Area 96.63%.

**2-(1-(5-Methyl-1-(4-(3-(3-methylpiperidin-1-yl)prop-1-yn-1-yl)phenyl)-1H-pyrazol-4-yl) ethylidene)hydrazine-1-carboximidamide (11).**

Yellowish-white solid (98 mg, 84.6%); mp = 187-189 °C. <sup>1</sup>H NMR (DMSO-*d*<sub>6</sub>) δ: 8.08 (s, 1H), 7.73 (d, *J* = 8.2 Hz, 2H), 7.12 (d, *J* = 8.2 Hz, 2H), 6.44 (brs, 4H), 3.62 (s, 2H), 2.68-2.57 (m, 4H), 2.39 (s, 3H), 2.32 (s, 3H), 1.65-1.57 (m, 5H), 0.92 (d, *J* = 6.2 Hz, 3H); <sup>13</sup>C NMR (DMSO-*d*<sub>6</sub>) δ: 154.3, 147.7, 142.8, 140.5, 138.2, 132.6, 127.5, 123.6, 122.7, 89.4, 81.6, 52.1, 41.1, 32.5, 29.3, 25.9, 19.6, 15.26; MS (*m/z*); 391 (M<sup>+</sup>, 100.00%). Anal. Calc. for: C<sub>22</sub>H<sub>29</sub>N<sub>7</sub> (391): C, 67.49; H, 7.47; N, 25.04; found; C, 68.06; H, 7.58; N, 24.97%. HPLC RT: 25.526; Area 95.63%.

**2-(1-(5-Methyl-1-(4-(3-(2-methylpiperidin-1-yl)prop-1-yn-1-yl)phenyl)-1H-pyrazol-4-yl) ethylidene)hydrazine-1-carboximidamide (12).** Yellowish-white solid (90 mg, 81.6%); mp = 185-187 °C. <sup>1</sup>H NMR (DMSO-*d*<sub>6</sub>) δ: 8.08 (s, 1H), 7.73 (d, *J* = 8.2 Hz, 2H), 7.12 (d, *J* = 8.2 Hz, 2H), 6.44 (brs, 4H), 3.62 (s, 2H), 2.68-2.57 (m, 4H), 2.39 (s, 3H), 2.32 (s, 3H), 1.65-1.57 (m, 5H), 0.92 (d, *J* = 6.2 Hz, 3H); <sup>13</sup>C NMR (DMSO-*d*<sub>6</sub>) δ: 154.3, 147.7, 142.8, 140.5, 138.2, 132.6, 127.5, 123.6, 122.7, 89.4, 81.6, 52.1, 41.1, 32.5, 29.3, 25.9, 19.6, 15.26; MS (*m/z*); 391 (M<sup>+</sup>, 100.00%). Anal. Calc. for: C<sub>22</sub>H<sub>29</sub>N<sub>7</sub> (391): C, 67.49; H, 7.47; N, 25.04; found; C, 68.06; H, 7.58; N, 24.97%. HPLC RT: 25.726; Area 95.83%.

**2-(1-(5-Methyl-1-(4-(3-(piperidin-1-yl)prop-1-yn-1-yl)phenyl)-1H-pyrazol-4-yl)ethylidene) hydrazine-1-carboximidamide (13).** Yellowish-white solid (102 mg, 87.6%); mp = 200-202 °C. <sup>1</sup>H NMR (DMSO-*d*<sub>6</sub>) δ: 8.04 (s, 1H), 7.71 (d, *J* = 8.2 Hz, 2H), 7.22 (d, *J* = 8.2 Hz, 2H), 6.44 (brs, 4H), 3.62 (s, 2H), 2.68-2.57 (m, 4H), 2.39 (s, 3H), 2.32 (s, 3H), 1.65-1.57 (m, 6H); <sup>13</sup>C NMR (DMSO-*d*<sub>6</sub>) δ: 154.3, 147.7, 142.8, 140.5, 138.2, 132.6, 127.5, 123.6, 122.7, 89.4, 81.6, 52.1, 41.1, 32.5, 29.3, 25.9, 15.26; MS (*m/z*); 377 (M<sup>+</sup>, 100.00%). Anal. Calc. for: C<sub>21</sub>H<sub>27</sub>N<sub>7</sub> (377): C, 66.82; H, 7.21; N, 25.97; found; C, 66.96; H, 7.28; N, 25.88%. HPLC RT: 24.226; Area 98.63%.

**2-(1-(1-(4-(3-((4-Hydroxyphenyl)amino)prop-1-yn-1-yl)phenyl)-5-methyl-1H-pyrazol-4-yl) ethylidene)hydrazine-1-carboximidamide (14).** Yellow solid (115 mg, 91.6%); mp = 210-212 °C. <sup>1</sup>H NMR (DMSO-*d*<sub>6</sub>) δ: 9.14 (brs, 1H), 8.08 (s, 1H), 7.74 (d, *J* = 8.2 Hz, 2H), 7.24 (d, *J* = 8.2 Hz, 2H), 7.17 (d, *J* = 8.2 Hz, 2H), 6.94 (d, *J* = 8.2 Hz, 2H), 5.48 (brs, 4H), 4.65 (brs, 1H), 3.62 (s, 2H), 2.39 (s, 3H), 2.32 (s, 3H); <sup>13</sup>C NMR (DMSO-*d*<sub>6</sub>) δ: 163.4, 158.7, 157.3, 146.3, 148.3, 144.5, 141.3, 138.5, 132.6, 127.3, 123.3, 122.2, 120.2, 115.2, 86.4, 81.4, 32.8, 30.1, 12.26; MS (*m/z*); 401 (M<sup>+</sup>, 100.00%). Anal. Calc. for: C<sub>22</sub>H<sub>23</sub>N<sub>7</sub>O (401): C, 65.82; H, 5.77; N, 24.42; found; C, 65.96; H, 5.88; N, 24.26%. HPLC RT: 21.326; Area 97.43%.

#### 4.2. Microbiological assays

**Bacterial strains, antibiotics, and compounds.** According to guidelines outlined by the Clinical and Laboratory Standards Institute (CLSI) or as described in previous reports, the minimum inhibitory concentrations (MICs) of the tested compounds and control drugs were determined using the broth microdilution method. (Citron and Hecht 2011, Elsebaei, Abutaleb et al. 2019, Shivanna and Dasegowda 2023, Atwa, Hagraas et al. 2024) We evaluated the antimicrobial properties of new phenylpyrazole derivatives against clinically relevant strains of MRSA, *E. coli*, *C. difficile*, and *N. gonorrhea*. At 37°C, *S. aureus* and *E. coli* were grown aerobically overnight on tryptone soy agar (TSA) plates. For 48 hours, *C. difficile* grew anaerobically on brain-heart infusion-rich agar at 37°C. On GC chocolate agar, *N. gonorrhoeae* was grown for 24 hours at 37°C with 5% CO<sub>2</sub>. On a yeast peptone dextrose (YPD) agar plate, a bacterial solution equal to 0.5 McFarland standard was prepared and diluted in cation-adjusted Mueller-Hinton broth (CAMHB) for *S. aureus* and *E. coli*. *C. difficile* was diluted in brain-heart infusion-supplemented broth to achieve a bacterial concentration of about 5 × 10<sup>5</sup> CFU/ml. *N. gonorrhoeae* was diluted in brucella broth supplemented with NAD, pyridoxal, hematin, neopeptone, and yeast extract to

achieve a bacterial concentration of about  $1 \times 10^6$  CFU/ml. Compounds and control drugs were added in the first row of the 96-well plates and serially diluted along the plates. Plates were incubated as previously described. (Geers and Donabedian 1989, Hagra, Abutaleb et al. 2020, Elsebaei, Mancy et al. 2022).

## REFERENCES

- Algammal, A. M., H. F. Hetta, A. Elkelish, D. H. H. Alkhalifah, W. N. Hozzein, G. E.-S. Batiha, N. El Nahhas and M. A. Mabrok (2020).** "Methicillin-Resistant Staphylococcus aureus (MRSA): one health perspective approach to the bacterium epidemiology, virulence factors, antibiotic-resistance, and zoonotic impact." Infection and drug resistance: 3255-3265.
- Aljohani, A. K., W. A. Z. El Zalwa, M. Alswah, M. A. Seleem, M. M. Elsebaei, A. H. Bayoumi, A. M. El-Morsy, M. Almaghrabi, A. A. Awaji and A. Hammad (2023).** "Development of Novel Class of Phenylpyrazolo [3, 4-d] pyrimidine-Based Analogs with Potent Anticancer Activity and Multitarget Enzyme Inhibition Supported by Docking Studies." International Journal of Molecular Sciences 24(19): 15026.
- Atwa, S. S., M. Hagra, A. S. Mayhoub and M. Elsebaei (2024).** "SYNTHESIS OF SOME NEW AZOLE DERIVATIVES AS ANTIBACTERIAL AGENTS." Al-Azhar Journal of Pharmaceutical Sciences 69(1): 108-129.
- Awaji, A. A., W. A. Z. El Zalwa, M. A. Seleem, M. Alswah, M. M. Elsebaei, A. H. Bayoumi, A. M. El-Morsy, M. Y. Alfaifi, A. A. Shati and S. E. I. Elbehairi (2024).** "N- and s-substituted Pyrazolopyrimidines: A promising new class of potent c-Src kinase inhibitors with prominent antitumor activity." Bioorganic chemistry 145: 107228.
- Burnham, C.-A. D., J. Leeds, P. Nordmann, J. O'Grady and J. Patel (2017).** "Diagnosing antimicrobial resistance." Nature Reviews Microbiology 15(11): 697-703.
- Citron, D. M. and D. W. Hecht (2011).** "Susceptibility test methods: anaerobic bacteria." Manual of clinical microbiology: 1204-1214.
- Eid, I., M. M. Elsebaei, H. Mohammad, M. Hagra, C. E. Peters, Y. A. Hegazy, B. Cooper, J. Pogliano, K. Pogliano and H. S. Abulkhair (2017).** "Arylthiazole antibiotics targeting intracellular methicillin-resistant Staphylococcus aureus (MRSA) that interfere with bacterial cell wall synthesis." European journal of medicinal chemistry 139: 665-673.

- El-Din, H. T. N., M. M. Elsebaie, N. S. Abutaleb, A. M. Kotb, A. S. Attia, M. N. Seleem and A. S. Mayhoub (2023).** "Expanding the structure–activity relationships of alkynyl diphenylurea scaffold as promising antibacterial agents." RSC Medicinal Chemistry 14(2): 367-377.
- El-Gamal, K., F. Sherbiny, A. El-Morsi, H. Abu-El-khair, I. Eissa and M. El-Sebaei (2015).** "Design, synthesis and antimicrobial evaluation of some novel quinoline derivatives." Pharm Pharmacol Int J 2(5): 165-177.
- Elbakry, O. M., M. F. Harras, M. M. Elsebaei, A. Mehany and H. Elsehrawi (2024).** "Development of pyrazolo [1, 5-a] pyrimidine derivatives: Synthesis, anticancer activity and docking study." Azhar International Journal of Pharmaceutical and Medical Sciences 4(1): 76-90.
- Elsebaei, M., A. Mancy, A. Mayhoub and M. Ayman (2022).** "DESIGN AND SYNTHESIS OF NOVEL TERREMIDE DERIVATIVES FOR PHARMACOLOGICAL EVALUATION." Al-Azhar Journal of Pharmaceutical Sciences 66(2): 87-98.
- Elsebaei, M. M., N. S. Abutaleb, A. A. Mahgoub, D. Li, M. Hagra, H. Mohammad, M. N. Seleem and A. S. Mayhoub (2019).** "Phenylthiazoles with nitrogenous side chain: an approach to overcome molecular obesity." European Journal of Medicinal Chemistry 182: 111593.
- Elsebaei, M. M., H. G. Ezzat, A. M. Helal, M. H. El-Shershaby, M. S. Abdulrahman, M. Alsedawy, A. K. Aljohani, M. Almaghrabi, M. Alsulaimany and B. Almohaywi (2024).** "Rational design and synthesis of novel phenyltriazole derivatives targeting MRSA cell wall biosynthesis." RSC advances 14(54): 39977-39994.
- Elsebaei, M. M., H. Mohammad, M. Abouf, N. S. Abutaleb, Y. A. Hegazy, A. Ghiaty, L. Chen, J. Zhang, S. R. Malwal and E. Oldfield (2018).** "Alkynyl-containing phenylthiazoles: Systemically active antibacterial agents effective against methicillin-resistant *Staphylococcus aureus* (MRSA)." European journal of medicinal chemistry 148: 195-209.
- Elsebaei, M. M., H. Mohammad, A. Samir, N. S. Abutaleb, A. B. Norvil, A. R. Michie, M. M. Moustafa, H. Samy, H. Gowher and M. N. Seleem (2019).** "Lipophilic efficient phenylthiazoles with potent undecaprenyl pyrophosphatase inhibitory activity." European journal of medicinal chemistry 175: 49-62.
- Elsebaie, M. M., H. T. N. El-Din, N. S. Abutaleb, A. A. Abuelkhir, H.-W. Liang, A. S. Attia, M. N. Seleem and A. S. Mayhoub (2022).** "Exploring the structure-activity relationships of diphenylurea as an antibacterial scaffold active against methicillin-



and vancomycin-resistant *Staphylococcus aureus*." European Journal of Medicinal Chemistry 234: 114204.

**Geers, T. A. and A. M. Donabedian (1989).** "Comparison of broth microdilution and agar dilution for susceptibility testing of *Neisseria gonorrhoeae*." Antimicrobial agents and chemotherapy 33(2): 233-234.

**Hagras, M., N. S. Abutaleb, N. M. Elhosseiny, T. M. Abdelghany, M. Omara, M. M. Elsebaei, M. Alhashimi, A. B. Norvil, M. I. Gutay and H. Gowher (2020).** "Development of biphenylthiazoles exhibiting improved pharmacokinetics and potent activity against intracellular *Staphylococcus aureus*." ACS Infectious Diseases 6(11): 2887-2900.

**Hammad, A., N. S. Abutaleb, M. M. Elsebaei, A. B. Norvil, M. Alswah, A. O. Ali, J. A. Abdel-Aleem, A. Alattar, S. A. Bayoumi and H. Gowher (2019).** "From phenylthiazoles to phenylpyrazoles: broadening the antibacterial spectrum toward carbapenem-resistant bacteria." Journal of medicinal chemistry 62(17): 7998-8010.

**Helal, A. M., A. M. Sayed, M. Omara, M. M. Elsebaei and A. S. Mayhoub (2019).** "Peptidoglycan pathways: there are still more!" RSC advances 9(48): 28171-28185.

**Hosny, Y., N. S. Abutaleb, M. Omara, M. Alhashimi, M. M. Elsebaei, H. S. Elzahabi, M. N. Seleem and A. S. Mayhoub (2020).** "Modifying the lipophilic part of phenylthiazole antibiotics to control their drug-likeness." European journal of medicinal chemistry 185: 111830.

**Hung, L.-W., H.-B. Kim, S. Murakami, G. Gupta, C.-Y. Kim and T. C. Terwilliger (2013).** "Crystal structure of AcrB complexed with linezolid at 3.5 Å resolution." Journal of structural and functional genomics 14: 71-75.

**Lee, A. S., H. De Lencastre, J. Garau, J. Kluytmans, S. Malhotra-Kumar, A. Peschel and S. Harbarth (2018).** "Methicillin-resistant *Staphylococcus aureus*." Nature reviews Disease primers 4(1): 1-23.

**Mancy, A., N. S. Abutaleb, M. M. Elsebaei, A. Y. Saad, A. Kotb, A. O. Ali, J. A. Abdel-Aleem, H. Mohammad, M. N. Seleem and A. S. Mayhoub (2019).** "Balancing physicochemical properties of phenylthiazole compounds with antibacterial potency by modifying the lipophilic side chain." ACS infectious diseases 6(1): 80-90.

**Mohammad, H., A. S. Mayhoub, A. Ghafoor, M. Soofi, R. A. Alajlouni, M. Cushman and M. N. Seleem (2014).** "Discovery and characterization of potent thiazoles

versus methicillin-and vancomycin-resistant Staphylococcus aureus." Journal of medicinal chemistry 57(4): 1609-1615.

**Nathan, C. (2020).** "Resisting antimicrobial resistance." Nature Reviews Microbiology 18(5): 259-260.

**Omara, M., M. Hagra, M. M. Elsebaie, N. S. Abutaleb, H. T. N. El-Din, M. O. Mekhail, A. S. Attia, M. N. Seleem, M. T. Sarg and A. S. Mayhoub (2023).** "Exploring novel aryl/heteroaryl-isosteres of phenylthiazole against multidrug-resistant bacteria." RSC advances 13(29): 19695-19709.

**Ornik-Cha, A., J. Wilhelm, J. Kobyłka, H. Sjuts, A. V. Vargiu, G. Mallocci, J. Reitz, A. Seybert, A. S. Frangakis and K. M. Pos (2021).** "Structural and functional analysis of the promiscuous AcrB and AdeB efflux pumps suggests different drug binding mechanisms." Nature Communications 12(1): 6919.

**Sayed, A. M., N. S. Abutaleb, A. Kotb, H. G. Ezzat, M. N. Seleem, A. S. Mayhoub and M. M. Elsebaie (2023).** "Arylpyrazole as selective anti-enterococci; synthesis and biological evaluation of novel derivatives for their antimicrobial efficacy." Journal of Heterocyclic Chemistry 60(1): 134-144.

**Shahin, I. G., K. O. Mohamed, A. T. Taher, M. M. Elsebaei, A. S. Mayhoub, A. E. Kassab and A. Elshewy (2023).** "New Phenylthiazoles: Design, Synthesis, and Biological Evaluation as Antibacterial, Antifungal, and Anti-COVID-19 Candidates." Chemistry & Biodiversity 20(11): e202301143.

**Shivanna, V. and V. Dasegowda (2023).** "Comparison of disk diffusion and agar dilution method for the detection of mupirocin resistance in staphylococcal isolates from skin and soft tissue infections." Journal of laboratory physicians 15.

**Sugden, R., R. Kelly and S. Davies (2016).** "Combating antimicrobial resistance globally." Nature microbiology 1(10): 1-2.

**Turner, N. A., B. K. Sharma-Kuinkel, S. A. Maskarinec, E. M. Eichenberger, P. P. Shah, M. Carugati, T. L. Holland and V. G. Fowler Jr (2019).** "Methicillin-resistant Staphylococcus aureus: an overview of basic and clinical research." Nature Reviews Microbiology 17(4): 203-218.

## تشديد بعض مشتقات الفينيل بيرازول الجديدة كمضادة للبكتيريا.

احمد عبدالناصر<sup>1,2</sup>، شريف فؤاد حماد<sup>3</sup>، عبد الرحمن صلاح ميهوب<sup>1,2</sup>، محمد مصطفى السباعي<sup>1</sup>.

<sup>1</sup>قسم الكيمياء العضوية الصيدلانية، كلية الصيدلة، جامعة الازهر، مدينة نصر، القاهرة، مصر.

<sup>2</sup>جامعة العلوم والتكنولوجيا، برنامج علوم النانو، مدينة زويل للعلوم والتكنولوجيا، حدائق أكتوبر الجيزة، مصر.

<sup>3</sup>معهد العلوم الأساسية والتطبيقية، الجامعة المصرية اليابانية للعلوم والتكنولوجيا، مدينة برج العرب الجديدة، الإسكندرية، مصر.

البريد الإلكتروني للباحث الرئيسي: [m.elsebaei@azhar.edu.eg](mailto:m.elsebaei@azhar.edu.eg)

تُعزى المركبات العضوية الصغيرة ذات الخصائص الشديدة المحبة للدهون غالبًا إلى سوء الخصائص الفيزيائية والكيميائية، مما يؤدي إلى تأثيرات جانبية غير مرغوب فيها وانخفاض فرص إجراء تجارب سريرية كاملة. لتحسين الخصائص الفيزيائية والكيميائية والسلوك الدوائي العام، تم تعديل هياكل المضادات الحيوية من نوع الفينيل بيرازول المستقرة ميتابوليكياً، والتي تتمتع بخصائص عالية المحبة للدهون بسبب مجموعة الألكاين، من خلال إدخال أمين حلقي في الذيل المحب للدهون. كانت المشتقات الألكاينية التي تحتوي على حلقات ذات 4 ذرات كربون حلقة هي الوحيدة التي أظهرت نشاطاً مضاداً للبكتيريا ملحوظاً. كان المركب الذي يحتوي على الأيزيتيدين هو الأكثر فعالية وأظهر نشاطاً مضاداً للبكتيريا معتدلاً ضد العقودية الذهبية المقاومة للميثيسيلي (MRSA) زاد الاستبدال بمشتق الأيزيتيدين من ملف قابلية الذوبان في الماء للمركب الجديد بشكل ملحوظ. حسن ذلك بشكل كبير الملف الدوائي للمركب، مع زيادة في نصف عمر المركب والوقت الذي كانت فيه تركيزاته في البلازما أعلى من الحد الأدنى لتركيز التنشيط (MIC) ضد MRSA. تم تحسين الملف الدوائي لهذه السلسلة الجديدة بنجاح مع الحفاظ على النشاط البيولوجي للمركبات ضد MRSA من خلال التعديلات على الفينيل بيرازول الألكاينية الموضحة هنا.

**الكلمات المفتاحية:** مقاومة المضادات الحيوية، البكتيريا متعددة المقاومة، المكورات العنقودية الذهبية المقاومة للميثيسيلين، الأمين الحلقي، تفاعل الاقتران المتقاطع سونوجاشيرا.